




ARTICLE

Selective effects of acute and chronic stress on slow and alpha-theta cortical functional connectivity and reversal with subanesthetic ketamine

Donovan M. Ashby^{1,2,3} and Alexander McGirr^{1,2,3} 

© The Author(s), under exclusive licence to American College of Neuropsychopharmacology 2022

Anxious, depressive, traumatic, and other stress-related disorders are associated with large scale brain network functional connectivity changes, yet the relationship between acute stress effects and the emergence of persistent large scale network reorganization is unclear. Using male Thy 1-jRGECO1a transgenic mice, we repeatedly sampled mesoscale cortical calcium activity across dorsal neocortex. First, mice were imaged in a homecage control condition, followed by an acute foot-shock stress, a chronic variable stress protocol, an acute on chronic foot-shock stress, and finally treatment with the prototype rapid acting antidepressant ketamine or vehicle. We derived functional connectivity metrics and network efficiency in two activity bands, namely slow cortical activity (0.3–4 Hz) and theta-alpha cortical activity (4–15 Hz). Compared to homecage control, an acute foot-shock stress induced widespread increases in cortical functional connectivity and network efficiency in the 4–15 Hz temporal band before normalizing after 24 h. Conversely, chronic stress produced a selective increase in between-module functional connectivity and network efficiency in the 0.3–4 Hz band, which was reversed after treatment with the rapid acting antidepressant ketamine. The functional connectivity changes induced by acute stress in the 4–15 Hz band were strongly related to those in the slow band after chronic stress, as well as the selective effects of subanesthetic ketamine. Together, this data indicates that stress induces functional connectivity changes with spatiotemporal features that link acute stress, persistent network reorganization after chronic stress, and treatment effects.

Neuropsychopharmacology (2023) 48:642–652; <https://doi.org/10.1038/s41386-022-01506-y>

INTRODUCTION

Anxiety, depression, and trauma-related disorders are highly prevalent and associated with significant morbidity and mortality [1]. These conditions are increasingly recognized as the result of alterations to neural circuitry caused by repeated stress [2], in particular, functional neuroimaging has identified persistent changes to large scale network in stress-related disorders [3–5]. Yet, it is uncertain how discrete acute stress events impact network connectivity, if at all. Tractable models can be used to investigate how acute and chronic stress are related in brain networks, and inform our mechanistic understanding of how persistent network alterations emerge in stress-related disorders.

Stress results in an ordered neurochemical cascade to appropriately respond to threat, however chronic activation of this response results in enduring behavioral and neurochemical changes that are used to model human conditions associated with stress, such as anxiety, depression, and trauma in tractable species [6]. At the cellular level, chronic activation of the stress response results in numerous changes that impact circuit function, including altered neurotransmission [7], dendritic arborization [8], as well as the development and maintenance of dendritic spines [9]. These are reflected in changes in the functional organization of large scale networks after chronic stress, as observed using

multiple modalities of brain activity measurement, including functional magnetic resonance imaging [10–12], electrophysiology [13], and mesoscale optical imaging [14].

There is limited data on the effects of acute stress on large-scale networks in both humans and tractable species. In model organisms, existing research has found changes in regional activity after the administration of exogenous corticosterone [15], but functional reorganization of brain wide networks has not been reported. In human imaging, the effects of acute stress have also principally been studied using a task based approach [16], with some notable exceptions that have shown transient changes in functional connectivity between functional networks [17], particularly the default mode and salience networks [18]. As these networks appear to be conserved between murine species and humans [19], and are susceptible to reorganization after chronic stress [14], it is plausible that network reorganization occurs transiently in response to a single acute stressor and that this may inform the persistent changes of chronic stress.

Mesoscale imaging using genetically encoded indicators of neuronal activity resolves certain methodological challenges to studying large scale networks in acute stress and how these relate to a chronic stress phenotype. Mesoscale imaging, combined with non-invasive chronic preparations [20] and fluorescent biosensors

¹Department of Psychiatry, University of Calgary, Calgary, AB, Canada. ²Hotchkiss Brain Institute, University of Calgary, Calgary, AB, Canada. ³Mathison Centre for Mental Health Research and Education, Calgary, AB, Canada. ✉email: alexander.mcgirr@ucalgary.ca

Received: 8 June 2022 Revised: 3 November 2022 Accepted: 6 November 2022

Published online: 19 November 2022

that sample directly coupled proxies of neural activity such as intracellular calcium [21] permit repeated sampling of neuronal activity over large expanses of cerebral cortex to describe large scale network structure changes [22]. Ongoing advances in genetically encoded calcium sensors have resulted in constructs with favorable tissue penetrance properties and that are less contaminated by hemodynamic intrinsic signal fluctuations [23, 24]. Here, we use mesoscale imaging of spontaneous cortical activity during quiet wakefulness in mice to align with human resting state functional magnetic resonance imaging, with the notable advantage that mesoscale calcium imaging affords greater temporal resolution to examine activity functional connectivity across different timescales of neural activity. We use repeated sampling of neuronal activity to characterize changes in large scale functional networks after acute stress, and how this instantiates a chronic stress phenotype. We then examine how rapid synaptogenesis with the rapid acting antidepressant ketamine [25, 26] relates to both acute and chronic stress phenotypes.

METHODS

Animals

Adult male C57BL/6J-Tg(Thy1-jRGECO1a)GP8.58Dkim/J mice (8–12 weeks old), constitutively expressing the red-shifted calcium indicator jRGECO1a under the Thy-1 promoter, were used for all experiments. Animals were group housed on a 12:12 light cycle with ad libitum access to food and water. All procedures were approved by the University of Calgary Animal Care Committee (ACC) in accordance with the ethical standards set forth by the Canadian Council on Animal Care (CCAC).

Complex and frequency-dependent sex differences have been identified when examining largescale network changes in rodent models of chronic stress [27]. Recognizing this complexity, before dissecting sex-specific effects we sought first to test whether functional connectivity changes as a result of acute stress ultimately inform the large scale reorganization that results from chronic stress, or whether these are unrelated. Here, we test this relationship in a single sex, however, the possibility of sexual dimorphism is extremely deserving of further study.

Drugs

Ketamine Hydrochloride (Ketalean, Bimeda-MTC, Canada) was dissolved in 0.9% saline and administered at a concentration of 10 mg/kg with intraperitoneal injection (IP) in a volume of 200 μ l.

Surgeries

Chronic window surgeries were performed in 7–8 week old mice as previously described [20]. Mice were isoflurane anesthetized (4% induction, 1.5–2.5% maintenance, 0.5 L/min oxygen) with buprenorphine (0.03 mg/kg) administered subcutaneously for analgesia. Body temperature was maintained at 37 °C, eyes were lubricated (Opticare, CLC Medica), and bupivacaine (Sterimax, intradermal, 0.05 mL) was administered locally at the excision site. Following disinfection with 3x alternating chlorhexidine (2%) and alcohol (70%), the skull was exposed with a skin excision from 3 mm anterior to bregma to 2 mm posterior to lambda, and bilaterally to the temporalis muscles. A metal screw was fix to the skull with cyanoacrylate prior to embedding in transparent dental cement (C&B-Metabond, Parkell). A flat 8 × 8 mm glass coverslip (tapered by 2 mm anteriorly) was fixed to the skull with transparent dental cement, taking care to avoid the formation of air pockets. Mice recovered for 7 days prior to further interventions, allowing for full cement hardening and wound healing.

Imaging protocol

Cortical calcium activity during quiet wakefulness was sampled using a LabeoTech system (Montreal, QC) employing a macroscope (Nikon 55 mm lens, f/2.8 aperture) and a Quantalux 2.1 MP Monochrome sCMOS Camera (Thorlabs). Using a 9.5 × 9.5 mm field of view capturing a large expanse of dorsal neocortex, we acquired 16-bit images with 19.7 ms temporal resolution (50 Hz) and 256 × 256 pixel resolution (26.2 px/mm). The genetically encoded calcium sensor, jRGECO1a, was excited with a 567 nm LED (540/80 filter, Semrock) attached to an articulating arm

(10–15 mW/cm²), and fluorescence emission was filtered with a 629/56 bandpass filter (Semrock). Focus was set ~500 mm below the cortical surface to minimize signal distortion from large blood vessels. Illumination and frame capture was controlled using commercial software (Labeo Technologies, Inc).

Mice were habituated to handling and head fixation with the embedded screw over 5 days prior to acquisitions. Epochs of 22,500 frames (7.5 min, 50 Hz) were sampled at predefined timepoints. For home cage, acute stress, and acute on chronic stress experiments, cortical activity was sampled at baseline, immediately after home cage control/footshock stress and then 1 h and 24 h after the intervention. We also sampled cortical activity after chronic variable stress (CVS), after pharmacological manipulation with subanesthetic vehicle/ketamine and 24 h after vehicle/ketamine administration.

Behavior protocol

For the acute stress condition, animals underwent a foot-shock stress drawn from the CVS protocol [28, 29]. Animals received 100 shocks (3 s, 0.4 mA) over 60 min delivered at random intervals using a shock generator (Shocker LE 100–26, Panlab) via stainless steel bar floors (Panlab) in a (19 W × 21 L × 13 H cm) foot-shock chamber.

A subset of animals underwent the CVS protocol [28, 29] to determine how chronic stress impacts functional connectivity. This protocol consists of twenty-one days over which one of three 1-h stressors are alternated to prevent habituation. The three stressors consist of foot-shock stress (100, 3 s, 0.4 mA shocks delivered at random intervals as above), tail suspension, and restraint in a 50 mL falcon tube. To determine whether acute stress resulted in a different pattern of functional connectivity changes after chronic stress, on the 21st day of the CVS protocol animals underwent an acute foot-shock stress with cortical activity sampling as per the acute stress protocol.

One day following completion of the CVS protocol, mice were assessed for a stress-related behavioral phenotypes on the open field test [30]. Briefly, mice were placed into a novel open field (40 × 40 × 60 cm) under ambient light conditions and allowed to freely explore for 10 min. Center of mass was tracked using an overhead camera and tracking software (ANYmaze, USA), and time in the arena center (A 29 × 29 cm square centered in the arena, representing ~50% of the arena) was computed as an index of stress-related behavior. One day following OFT, mice were tested for novelty suppressed feeding [31]. Mice were food restricted for 16 h prior to being placed in a novel habitat (28 × 18 × 12 cm) with clean bedding and lab chow (LabDiet, USA). Mice were recorded with an overhead camera (ANYmaze, USA) for offline scoring, and latency to feed was taken as an index of stress-related behavior.

Four days after completion of CVS, chronically stressed animals were imaged prior to and 24 h after treatment with a subanesthetic dose of ketamine (10 mg/kg IP), which has been shown to rapidly reverse behavioral and network level effects of chronic stress [14], or a vehicle control.

Image analysis

Image stacks were analyzed using custom-written MATLAB code (Mathworks, MA). Cortical activity during quiet wakefulness was expressed as change in fluorescence over the mean pixel fluorescence across the recording ($\Delta F/F_0$). Individual time-varying pixel signals were filtered in the slow (0.3–4 Hz) and theta/alpha (4–15 Hz) band for analysis. Movement episodes during imaging were identified as frames with outlier deviations in image mean square error from a spatially highpass filtered median image. Error frames constituted ~10% of frames in most recordings. Image stacks were rigidly aligned to the Allen Institute for Brain Science mouse brain atlas using five anatomical landmarks (the boundaries and midpoint where olfactory bulb meets cortex, bregma, and the base of retrosplenial cortex), and one functional landmark (primary sensory hindlimb region).

Functional connectivity analysis

Fifteen bilateral cortical ROIs (11 × 11 pixels, 420 × 420 μ m) were selected for a total of 30 ROIs based on a rigid alignment to the Allen atlas. Correlation matrices were created based on the zero-lag Pearson correlation of ROI pairs. Modules were identified using Louvain sorting on the averaged correlation matrix pooled from all baseline recordings, and the same module identity was used for all subsequent analysis. Gamma value and module number for Louvain sorting was chosen to maximize the number of modules while minimizing the number of

singleton/doublet modules that contained only one region bilaterally. To experimentally derive this value, individual baseline recordings were Louvain sorted at a range of gamma values, and the difference between total and singleton/doublet modules was calculated (Fig. S1). Connectivity changes were calculated as a difference from baseline, normalized to the baseline strength for each connection. To visualize network changes as a result of the behavioral protocol, differences in the average matrices were plotted as an undirected network diagram using modified code from the Bioinformatics and Brain Connectivity Toolbox [32]. To facilitate visualization, each connection was only represented if the correlation change was $\pm 10\%$ of the baseline condition. Average connectivity change was calculated as a mean across connections for each recording. Within-module connections and between-module connections were considered separately. Two-way repeated measures ANOVA was used to calculate significant differences in average connectivity between groups and across time. Significant interactions were followed up by post-hoc pairwise comparisons. Network efficiency was calculated for each recording (Bioinformatics and Brain Connectivity Toolbox [32]). Two-way repeated measures ANOVA was used to calculate significant differences in network efficiency between groups and across time. Huynh-Feldt corrected p -values are reported where sphericity assumption was violated.

For linear classification, network connectivity changes from each connection (435 edges) were used as response variables, with changes from each mouse as observations in the fitlinear function (MATLAB). Changes after acute stress and changes after the non-stress homecage control were used as the two training classes, and changes after chronic stress vs a non-stress control were used as the test data. Randomized group identities ($n = 100,000$ permutations) were used generate a null distribution for classification accuracy.

RESULTS

Mesoscale cortical Thy1-jRGECO1a imaging revealed activity dynamics over a wide expanse of dorsal neocortex, and 15 ROIs per hemisphere were identified based on alignment to the Allen Brain Atlas common coordinate framework [33], (Fig. 1a). Spontaneous calcium dynamics during quiet wakefulness were readily observed at multiple timescales and we focused on slow (0.3–4 Hz) and theta-alpha (4–15 Hz) bands. Calcium dynamics outside these temporal bands were either too slow to be accurately sampled with our chosen recording duration, or too fast to be captured due to temporal limitations in the calcium sensor. Activity fluctuations in each ROI were zero-lag correlated to produce a functional connectivity matrix for each power band.

To identify modules, the average baseline functional connectivity matrix in the 4–15 Hz band was Louvain sorted [32]. Module discovery based on Louvain sorting is highly dependent on the chosen gamma value, with higher gamma values resulting in more modules. At the limit, a single module may be discovered, or each ROI may be discovered as its own module. We sought to experimentally determine a gamma value that maximized the number of total modules discovered while minimizing the number of singleton/doublet modules that contained only a single ROI bilaterally. To this end, each baseline recording ($N = 17$) was sorted at a range of gamma values and modules numbers (total and singleton/doublet) were determined (Fig. S1). For all baseline recordings, 5 or 6 total modules, with gamma values clustering around 1.1, optimized our criteria. The average baseline functional connectivity matrix was subsequently sorted using these experimentally determined parameters, producing 5 modules that were used for all subsequent analyses (Fig. 1a). All modules included bilateral regions, reflecting the largely symmetrical activity patterns present during resting state [34]. Two larger modules encompassed 10 (5 bilateral regions), and 12 (6 bilateral regions) ROIs, identifiable as an anterior sensorimotor module and a posterior associational module. Two unitary bilateral modules, the anterior cingulate (ACC) and the sensory barrel field (S1BF) emerged. The final four-region module consisted of the motor and sensory hindlimb regions. These modules were highly conserved between animals, with consistent sorting of most edges in most mice (Fig. S1). The least consistent sorting was from

lateral parietal and visual cortex ROIs that would sort with the S1BF field in a minority of mice. A representative montage of slow spontaneous calcium dynamics over 2 s is illustrated in Fig. 1b. Figure 1c shows the average baseline functional connectivity as a connectivity matrix from $N = 17$ mice in the 0.3–4 Hz band, and this is represented as a biograph limited to the strongest 25% of edges in Fig. 1d (within-module connections) and Fig. 1e (between-module connections).

A representative montage of theta-alpha spontaneous calcium dynamics over two hundred milliseconds is illustrated in Fig. 1f. The Louvain sorted zero lag functional connectivity matrix is illustrated in Fig. 1g from the same $n = 17$ mice, and the associated biograph in Fig. 1h (within-module connections) and Fig. 1i (between-module connections). Baseline functional connectivity was broadly higher in the 0.3–4 Hz frequency band relative to the 4–15 Hz band (Fig. S2), although the mostly strongly connected edges were similar in both bands, and edges within the anterior sensorimotor module were similar between frequency bands.

Frequency dependent effects of acute stress on cortical functional connectivity

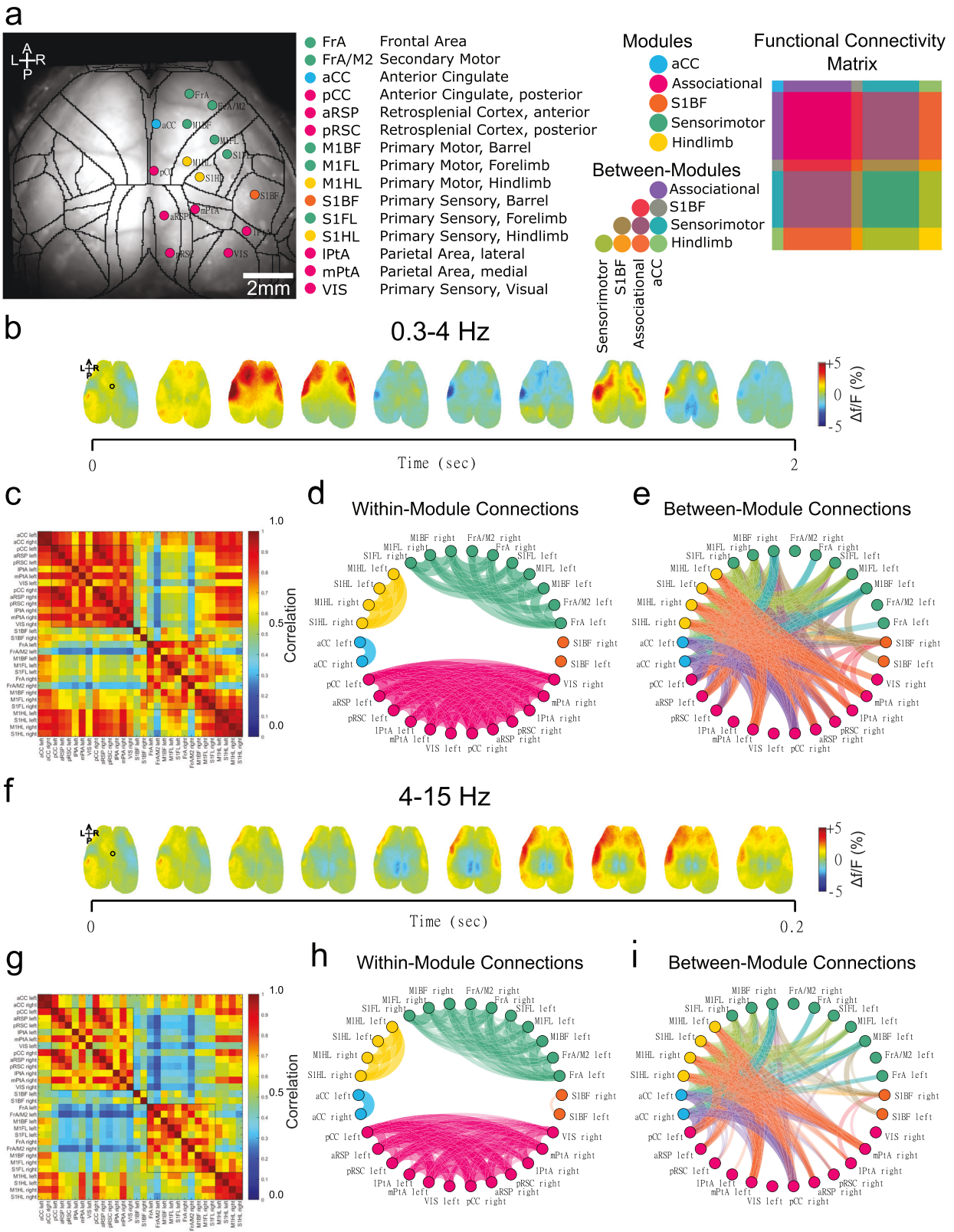
Compared to a homecage control condition, repeated imaging after acute stress (Fig. 2a) revealed temporal band specific changes in functional connectivity. In the 0.3–4 Hz band, average functional connectivity decreased in both stress and control groups with repeated imaging, while no significant difference was observed between groups (Figs. 2b–d, S3; within-modules ANOVA $F_{time(2,62)} = 9.26$, $p < 0.001$; $F_{group(1,62)} = 1.18$, $p = 0.29$; $F_{time*group(2,62)} = 0.66$, $p = 0.52$; between-modules ANOVA $F_{time(2,62)} = 19.14$, $p < 0.001$; $F_{group(1,62)} = 2.24$, $p = 0.14$; $F_{time*group(2,62)} = 2.58$, $p = 0.084$). Similarly, network efficiency decreased across recordings with no significant difference between groups (Fig. 2h; $F_{time(2,62)} = 4.02$, $p < 0.05$; $F_{group(1,62)} = 3.48$, $p = 0.072$; $F_{time*group(2,62)} = 1.09$, $p = 0.32$).

In the 4–15 Hz band, acute stress produced a significant increase in functional connectivity relative to control (Figs. 2e–g, S3), both within ($F_{time(2,62)} = 9.98$, $p < 0.001$; $F_{group(1,62)} = 14.50$, $p < 0.001$; $F_{time*group(2,62)} = 10.71$, $p < 0.001$) and between ($F_{time(2,62)} = 24.23$, $p < 0.001$; $F_{group(1,62)} = 11.24$, $p < 0.01$; $F_{time*group(2,62)} = 15.55$, $p < 0.001$) modules. This was associated with increased network efficiency (Fig. 2i; $F_{time(2,62)} = 22.16$, $p < 0.001$; $F_{group(1,62)} = 12.78$, $p < 0.01$; $F_{time*group(2,62)} = 13.75$, $p < 0.001$).

Post-hoc analysis indicated that this increase occurred immediately (within-modules, $t(31) = -4.66$, $p < 0.001$; between-modules $t(31) = -4.51$, $p < 0.001$; efficiency $t(31) = -4.74$, $p < 0.001$) and at 1 h after stress (within-modules $t(31) = -2.63$, $p < 0.05$; between-modules $t(31) = -2.34$, $p < 0.05$; efficiency $t(31) = -2.46$, $p < 0.05$), before returning to baseline after 24 h (within-modules $t(31) = -1.81$, $p = 0.08$; between-modules $t(31) = -1.09$, $p = 0.28$; efficiency $t(31) = -1.46$, $p = 0.16$). This data indicates that acute stress produces a broad increase in cortical functional connectivity at 4–15 Hz that persists for at least 1 h and returns to baseline at 24 h.

Frequency dependent effects of chronic variable stress on cortical functional connectivity

Next, mice underwent a chronic variable stress protocol (CVS), in which a rotating stressor was presented for 1 h each day for 21 days (Fig. 3a). Behavioral assays confirmed a depression-like phenotype in CVS mice as compared with control mice (Fig. 3b, OFT center time $t(19) = -3.23$, $p < 0.01$, novelty suppressed feeding $t(17) = 2.16$, $p < 0.05$). After completion of the CVS protocol, mice were imaged in the absence of an acute stressor to determine whether baseline functional connectivity was altered. This resulted in behavioral changes consistent with chronic stress, namely anxiety-like behavior as measured by time in the center of the



open field arena and latency in the novelty suppressed feeding test (Fig. 3b). In the 0.3–4 Hz band, functional connectivity was elevated both within modules (Figs. 3c, S4; $t(19) = -3.80, p < 0.01$) and between modules ($t(19) = -2.21, p < 0.05$) relative to a control group. Similarly, network efficiency was increased (Fig. 3d;

$t(19) = 2.25, p < 0.05$). As a subset of CVS mice did not show an increase in 0.3–4 Hz network efficiency, we asked whether this variability could be explained by an altered behavioral phenotype, possibly representing resilience to stress [35]. However no difference between CVS mice with decreased and increased

Fig. 1 Mesoscale cortical imaging in Thy-1 jRGECO1a mice. **a** Example raw image of the dorsal cortex during imaging. 15 ROIs per hemisphere were identified. ROIs are colored based on emergent groupings from Louvian sorting of average connectivity matrix in the 4–15 Hz band, with an exemplar color-coded functional connectivity matrix. **b** Example activity montage over 2 s. 10 frames are plotted, with calcium activity expressed as a change in relative fluorescence (df/F). **c** Functional connectivity matrix in the 0.3–4 Hz band. ROIs are ordered based on Louvian sorting. **d, e** Undirected weighted graph of functional connectivity in the 0.3–4 Hz band, colored based on Louvian sorting. For clarity only the top 25% of edge connections are plotted, showing within-module connections (**d**) and between-module connections (**e**). **f** Example activity montage over 200 msec. Functional connectivity matrix in the 4–15 Hz band (**g**). Undirected weighted graph of functional connectivity in the 4–15 Hz band. For clarity only the top 25% of edge connections are plotted, showing within-module connections (**h**) and between-module connections (**i**).

network efficiency was observed on the OFT ($t(13) = 0.23$, $p = 0.82$), or novelty-suppressed feeding ($t(11) = 0.16$, $p = 0.88$, Fig. S5). In contrast, in the 4–15 Hz band, no significant changes were observed (Figs. 3e, S4; within-modules, $t(19) = -1.44$, $p = 0.16$; between-modules, $t(19) = 1.18$, $p = 0.25$; Fig. 3f; efficiency $t(19) = -0.96$, $p = 0.35$). A non-significant trend for increased functional connectivity in between-module connections the 4–15 Hz band in control mice (Fig. S4) may have represented a mild stressor effect, due to a loss of habituation to head fixation during imaging across the 21 day procedure. These results are consistent with prior reports of increased functional connectivity after chronic stress paradigms in mice [14], and suggest that higher activity band connectivity changes get instantiated into lower activity bands with repeated stress.

Similarities between acute and chronic effects of stress on cortical functional connectivity

To determine whether connectivity changes during acute stress predict the change observed after chronic stress, cross-animal average connectivity change was correlated between acute and chronic stress for each edge connection. A general linear mixed effects regression model indicated a 3-way interaction between acute stress timepoint, frequency band, and within/between module identity. As acute stress changes were restricted to the 4–15 Hz band, and chronic stress changes to the 0.3–4 Hz band, we focused on this cross-band relationship, with analyses performed separately for between- and within-modules. Examining within-module connectivity, the effects immediately after stress showed a strong relationship with chronic stress (Fig. 4a; $r = 0.53$, $p < 0.001$), and was no longer significant an hour after stress (Fig. 4b; $r = 0.03$, $p = 0.74$). Between-module connectivity, however, showed persistent relationships between the effects of acute stress and those of CVS immediately after stress (Fig. 4c; $r = 0.80$, $p < 0.001$) and 1 h after stress (Fig. 4d; $r = 0.67$, $p < 0.001$). These results suggest that transient functional connectivity changes immediately after acute stress are highly predictive of the sustained changes in functional connectivity after chronic stress. To directly test the predictive utility changes following acute stress, a linear classifier model was trained on network changes after acute stress (vs control) in the 4–15 Hz band and used to predict group identity from network changes after chronic stress in the 0.3–4 Hz band. Connectivity changes immediately after acute stress accurately predicted 75% of group identities in chronic stress (Fig. 4e; $p < 0.001$), while connectivity changes 1 h after stress were not significantly predictive of group identities after chronic stress (Fig. 4f; $p = 0.14$).

Effects of acute stress challenge after chronic variable stress on cortical functional connectivity

We next sought to determine whether chronic stress altered the network response to an acute stress challenge. Animals having completed the CVS protocol were therefore imaged before and after a 1 h foot-shock stress and compared with the effects of the same acute stress on naïve mice. Acute stress in CVS mice was associated with a broad decrease in functional connectivity in the 0.3–4 Hz band (Fig. S6; within-module connections, $F_{time}(2,64) = 14.01$, $p < 0.001$; $F_{group}(1,64) = 1.51$, $p = 0.23$; $F_{time*group}(2,64) =$

2.97 , $p = 0.058$; between-module connections, $F_{time}(2,64) = 18.3$, $p < 0.001$; $F_{group}(1,64) = 1.23$, $p = 0.28$; $F_{time*group}(2,64) = 5.15$, $p < 0.01$). Post hoc analysis after significant time by group interactions indicated that chronic stress produced a larger decrease in connectivity strength in “between-module” connections in the 0.3–4 Hz band immediately after acute stress as compared with naïvely stressed mice ($t(32) = 2.27$, $p < 0.05$). Network efficiency was similar between CVS and naïve mice, with decreased efficiency in the 0.3–4 Hz band after acute stress ($F_{time}(2,64) = 4.48$, $p < 0.05$; $F_{group}(1,64) = 0.37$, $p = 0.54$; $F_{time*group}(2,64) = 3.52$, $p = 0.052$).

An increase in functional connectivity in the 4–15 Hz band (Fig. S6, within-module connections $F_{time}(2,64) = 37.40$, $p < 0.001$; $F_{group}(1,64) = 0.10$, $p = 0.76$; $F_{time*group}(2,64) = 0.76$, $p = 0.47$; between-module connections $F_{time}(2,64) = 41.13$, $p < 0.001$; $F_{group}(1,64) = 1.66$, $p = 0.21$; $F_{time*group}(2,64) = 1.01$, $p = 0.37$) was observed in both CVS and naïve mice, with no significant differences between groups. Increased network efficiency in the 4–15 Hz band was similar between groups ($F_{time}(2,64) = 41.60$, $p < 0.001$; $F_{group}(1,64) = 0.89$, $p = 0.35$; $F_{time*group}(2,64) = 0.75$, $p = 0.47$) after stress. Taken overall, the minimal differences between naïvely stressed and chronically stressed mice in response to an acute stress challenge indicate that functional connectivity changes after acute stress remain intact and unchanged after chronic stress.

Ketamine produces treatment and frequency dependent changes in cortical functional connectivity

Subanesthetic ketamine leads to rapid improvements in depressive symptoms in patients with major depressive disorder [36]. In animal models it similarly leads to rapid reversal of behaviors related to chronic stress [37] and normalization of cortical functional hyperconnectivity in the slow band associated with chronic stress [14]. After CVS, mice were treated with a subanesthetic dose of ketamine (Fig. 5a). After 24 h, ketamine reduced functional connectivity of between-module connections in the 0.3–4 Hz band as compared with a vehicle control group (Figs. 5b, S7; within-module connections, $t(14) = 2.45$, $p < 0.05$), while within-module connection changes were not significantly different between groups (Fig. S7; $t(14) = 1.75$, $p = 0.102$). Global efficiency was similarly reduced (Fig. 5c; $t(14) = 2.54$, $p < 0.05$). In the 4–15 Hz band, functional connectivity was not significantly reduced in within-module connections (Figs. 5d, S7; $t(14) = 1.85$, $p = 0.08$), between-module connections ($t(14) = 1.39$, $p = 0.19$) or global efficiency (Fig. 5e; $t(14) = 1.80$, $p = 0.09$).

Next, we examined whether ketamine’s effects were specific to the functional connectivity changes that were induced by chronic stress. We focused on the 0.3–4 Hz band where the effects of both CVS and ketamine were most pronounced. Functional connectivity changes were strongly correlated for within-module connections (Fig. 5f; $r = -0.68$, $p < 0.001$), and strongly correlated for between-module connections (Fig. 5g; $r = -0.89$, $p < 0.001$). As acute stress produced functional connectivity changes in the 4–15 Hz band that were correlated with CVS changes in the 0.3–4 Hz band, we examined whether ketamine acted on a correlated set of connections. We correlated the effects of ketamine in the 0.3–4 Hz band to the immediate effects of acute stress in

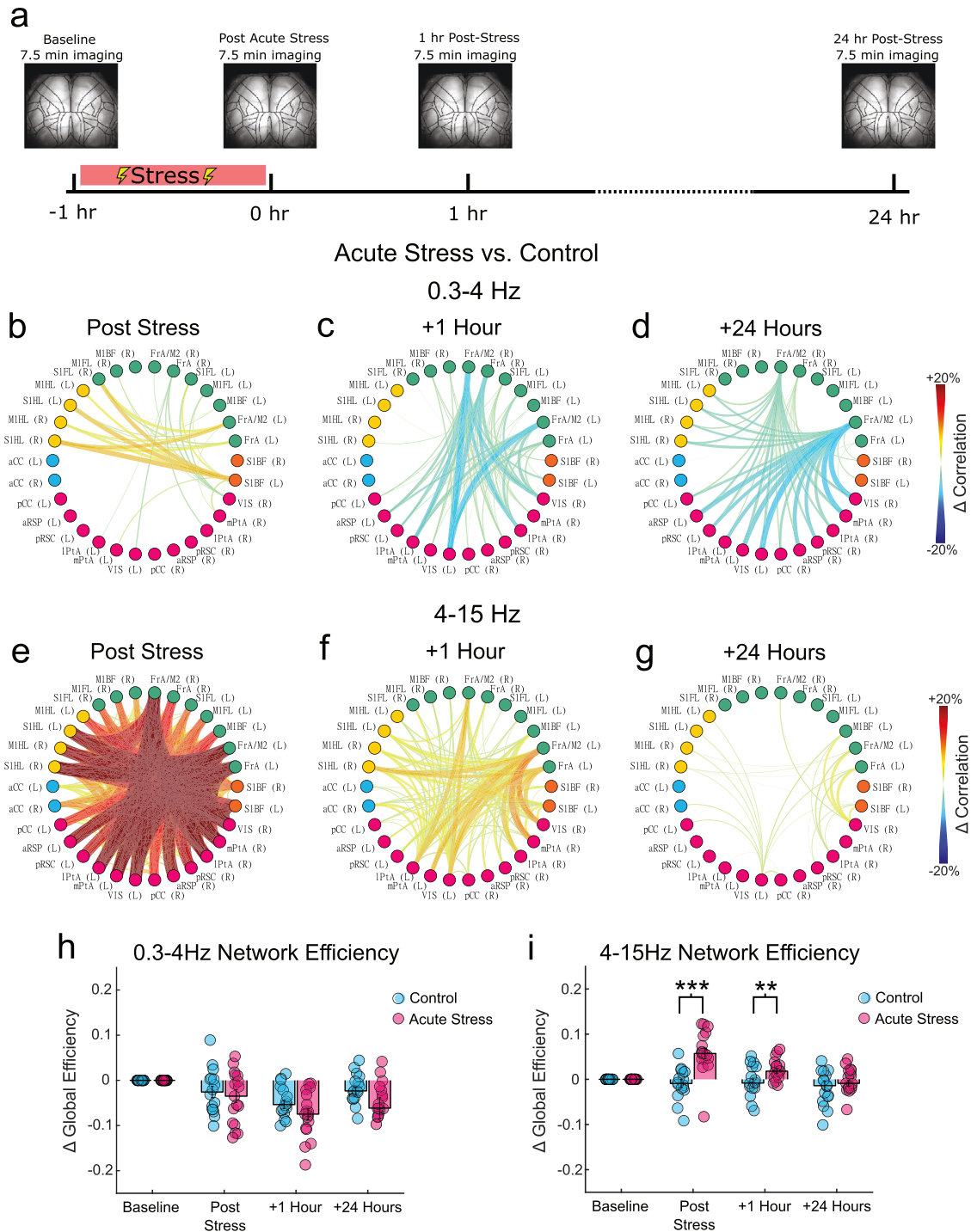


Fig. 2 Acute foot-shock stress elevates functional connectivity in the 4–15 Hz band. **a** Experiment diagram, illustrating repeated imaging sessions before and immediately, 1 h, and 24 h after a 1 h footshock stress. **b–d** Biograph displaying the difference between acute stress ($n = 17$) versus control ($n = 16$) in the change in strength of ROI connections in the 0.3–4 Hz band versus baseline (difference in acute stress). Only edges where this difference exceeded 10% are displayed, and edge thickness and color scales with difference between groups. No significant change was observed between acute stress and control in the 0.3–4 Hz band. **e, f** Biograph displaying the difference between acute stress versus control in the change in strength of ROI connections in the 4–15 Hz band versus baseline. Both within-module and between-module connections were significantly elevated in stress relative to control immediately (**e**) and 1 h after stress (**f**). **h** Global efficiency of the network decreased in both acute stress and control mice, with no significant difference between groups at any timepoints. **i** Global efficiency of the network increased in acute stress relative to control mice immediately after stress and at 1 h after stress. ($*p < 0.05$, $**p < 0.01$, $***p < 0.001$ follow-up pairwise comparison).

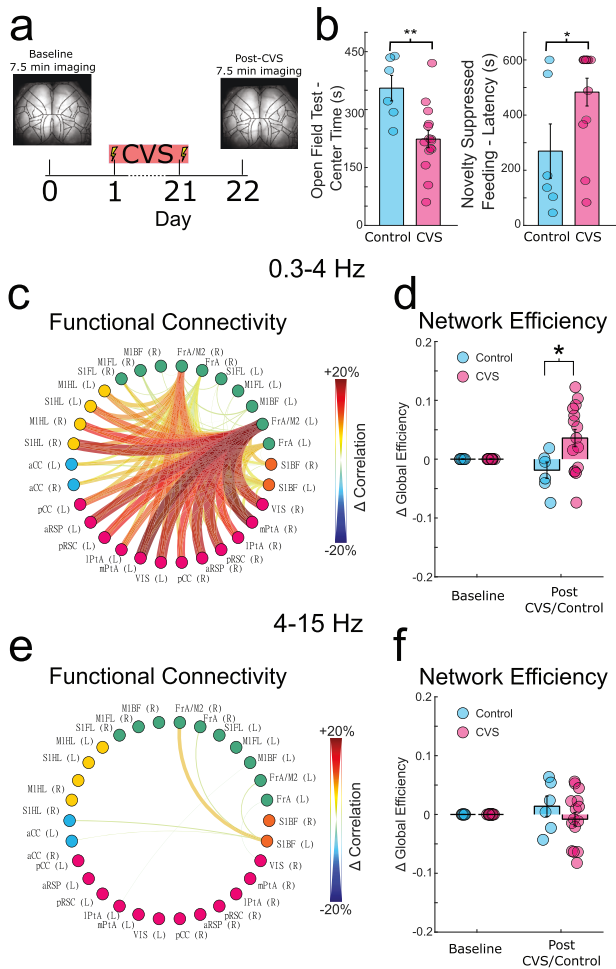


Fig. 3 Chronic variable stress elevates functional connectivity in the 0.3–4 Hz band. **a** Experiment diagram. Mice received a baseline imaging session prior to 21 daily stressors. 24 h after the final stressor mice were imaged for a post-stress session. **b** The CVS protocol resulted in stress-related anxiety-like behavioral changes, specifically time exploring the center of the arena on the open field test and latency to feed on the novelty suppressed feeding task. **c** Biograph displaying the change in strength of connections in the 0.3–4 Hz band after CVS ($n = 15$) relative to baseline. Both within-module and between-module connections were significantly increased. **d** Global efficiency of the network was significantly increased after chronic variable stress in the 0.3–4 Hz band, relative to a control ($n = 6$). **e** Biograph displaying the change in strength of connections in the 4–15 Hz band after CVS relative to baseline. No significant changes were observed. **f** Global efficiency of the network was unchanged in the 4–15 Hz band after CVS relative to a control. (* $p < 0.05$, ** $p < 0.01$, *** $p < 0.001$ follow-up pairwise comparison).

4–15 Hz band. Both within module (Fig. 5h; $r = -0.87, p < 0.001$) and between module connections (Fig. 5i; $r = -0.89, p < 0.001$) were highly inversely correlated. This indicates that ketamine’s effects on functional connectivity appear to be selective to the functional connections that exhibit rapid shifts with acute stress in the theta-alpha range and become persistent in the slow band after chronic stress. The full set of timepoint, band, and module specific correlations is available for chronic stress in Fig. S8 and for acute stress in Fig. S9.

DISCUSSION

Here, we report that acute and chronic stress produce frequency dependent alterations in functional connectivity during quiet

wakefulness. These frequency dependent changes exhibit predictive relationships as changes in one activity band after acute stress become instantiated in another after chronic stress. Moreover, treatment effects with the prototype rapid acting antidepressant, ketamine, appear to be selective to the changes that occur after acute and chronic stress.

After foot-shock stress, functional connectivity was elevated immediately and 1 h after cessation of the stress, with recovery after 24 h. This elevated functional connectivity was widespread, but pronounced in “between-module” connections, i.e., those more weakly connected nodes at baseline. This functional connectivity elevation was prominent in the 4–15 Hz band, which encompasses theta and alpha band oscillations, whereas in the slow band (0.3–4 Hz), a qualitative but statistically non-significant reduction in connectivity was observed. With 21 days of repeated variable stressors, baseline functional connectivity was elevated in the slow band, while no significant change was observed in 4–15 Hz band. When these chronically stressed mice were exposed to an acute stress challenge, functional connectivity elevated in the 4–15 Hz band similar to naïve mice. Administration of ketamine to chronically stressed mice produced a profound reduction in baseline functional connectivity 24 h later, reversing the hyperconnectivity produced by CVS.

While a significant decrease in functional connectivity was observed in the 0.3–4 Hz band in response to acute stress, this change was not specific to stress and was also observed in homecage control mice. As all imaging sessions involve restraint for the duration of imaging, it is possible that, despite prior habituation, the baseline imaging sessions in control mice constitute a mild stressor that provokes connectivity changes observable with subsequent imaging. Thus a transient decrease in functional connectivity in the 0.3–4 Hz band may be a consequence of even mild stress, while only more pronounced stress produces functional connectivity increases in higher frequency bands.

This study adds to an expanding body of work showing that chronic stress alters functional connectivity in the rodent brain, typically by elevating the strength of weakly connected regions [10, 12, 14]. This change is observed with different stress paradigms and different modalities of brain activity measurement. Here we show that CVS [6], a commonly used model of chronic stress with relevance to anxiety-like and depression-like phenotypes similarly produces an increase in functional connectivity that is specific to the slow band. Notably, we show that a single acute stress experience is sufficient to increase functional connectivity, although some differences are apparent. First, the connectivity change is observed primarily in a higher activity band (4–15 Hz), while changes in the slow band were smaller and comprised a reduction in connectivity. Second, this change is transient, returning close to baseline after 24 h. The neurobiological response to an acute stressor is typically viewed as adaptive, readying the organism for robust behavioral responses to adverse events. Consistent with this general function, enhance cortical connectivity, wherein weakly connected cortical regions become more strongly connected may serve to enhance response readiness during behavioral quiescence.

As acute stress produced functional connectivity elevation in a different, higher frequency band than chronic stress, one interpretation is that this connectivity change after acute stress is necessary for subsequent instantiation of more enduring changes in the slow band due to CVS. Our evidence that the connections that change most strongly are common between acute and chronic stress support this idea, however dissociation of a frequency dependent effect requires additional investigation to determine causality. The transience of the 4–15 Hz effect indicates that it may reflect rapid and limited components of the stress response, such as the catecholaminergic response to stress, meanwhile the changes in the slow frequency band suggests

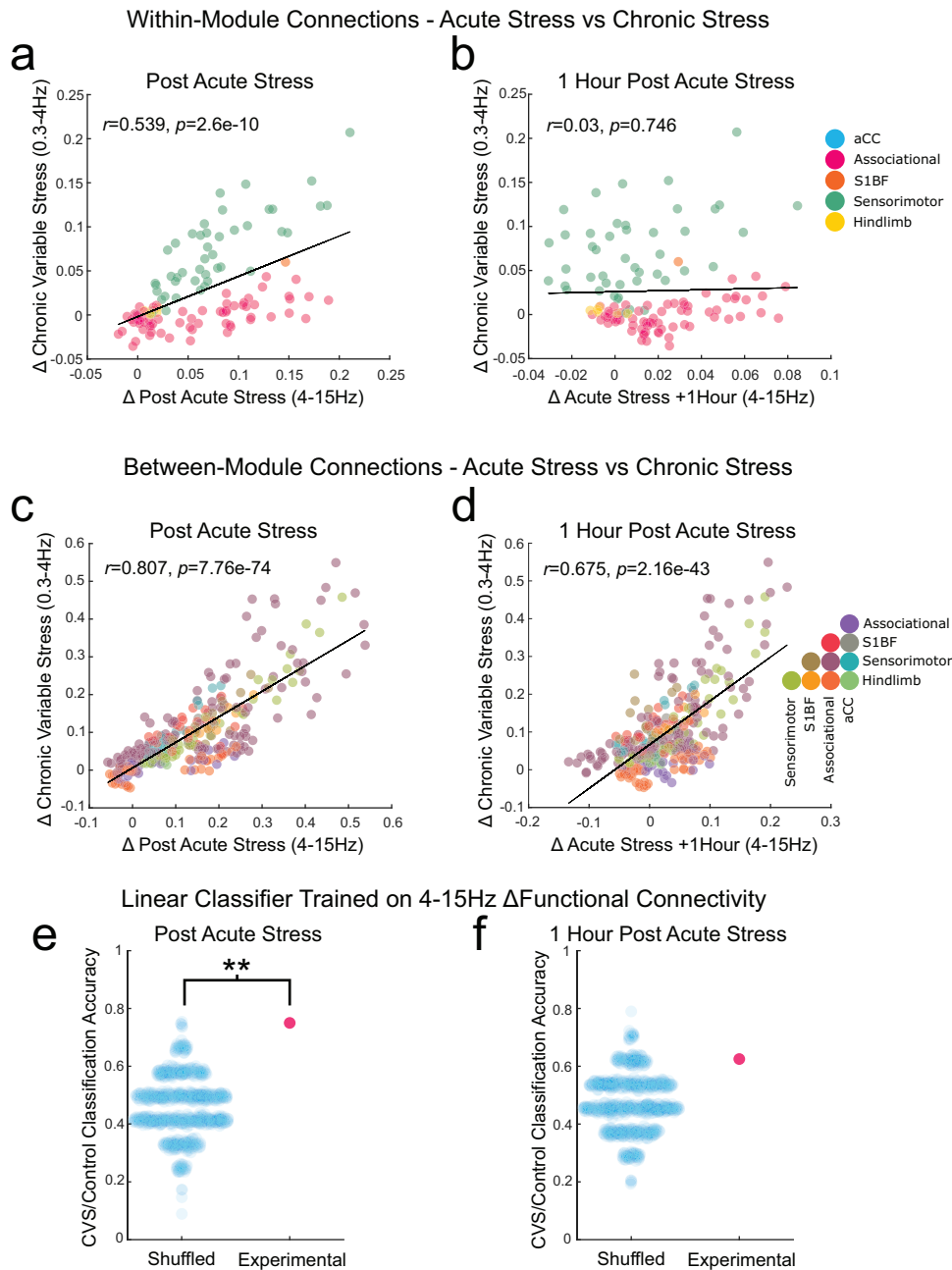


Fig. 4 Correlation between Acute Stress and Chronic Stress connectivity changes. **a** Comparing 4–15 Hz changes immediately after acute stress with 0.3–4 Hz changes after chronic stress, within-module connections were highly correlated. A single correlation was calculated using all within-module connections, colors indicate modules. **b** 1 h post stress, connectivity changes in response to acute stress are not correlated with changes observed after chronic stress. Between-modules, connectivity changes in the 4–15 Hz band both immediately (**c**) and 1 h (**d**) after acute stress are highly correlated with changes observed after chronic stress in the 0.3–4 Hz band. A linear classifier trained on acute stress functional connectivity changes significantly predicted (**e**) chronic stress changes vs a homecage control using changes immediately after stress, (**f**) but not changes 1 h after stress. (* $p < 0.05$, ** $p < 0.01$, *** $p < 0.001$ Pearson correlation).

that structural remodeling is required important [38], though still within the same circuitry.

While CVS produced behavioral alterations consistent with increased anxiety, we found no evidence that variability on center time in an open field test or latency to feed in a novelty suppressed feeding test was associated with variability in functional connectivity change in CVS mice. The possibility remains that a broader battery of behavioral assays that encompass different elements of a depression-like phenotype in mice may identify a subset of behavioral changes that covary with the magnitude of cortical functional connectivity change.

Considering the temporal profile of the jRGECO1a sensor [24] and our acquisition rate (50 Hz), our approach has several spatiotemporal advantages by capturing cortical activity at higher temporal scales than fMRI, but comes at the expense of characterizing brain regions not in the field of view. Moreover infraslow and higher frequency brain activity bands (notably gamma band activity and high frequency oscillations) are not captured by our approach. Despite these remaining limitations, our results emphasize the importance of measuring brain activity at multiple temporal scales, as a major stress-induced alteration in network activity would be unobservable if constrained to a single frequency band.

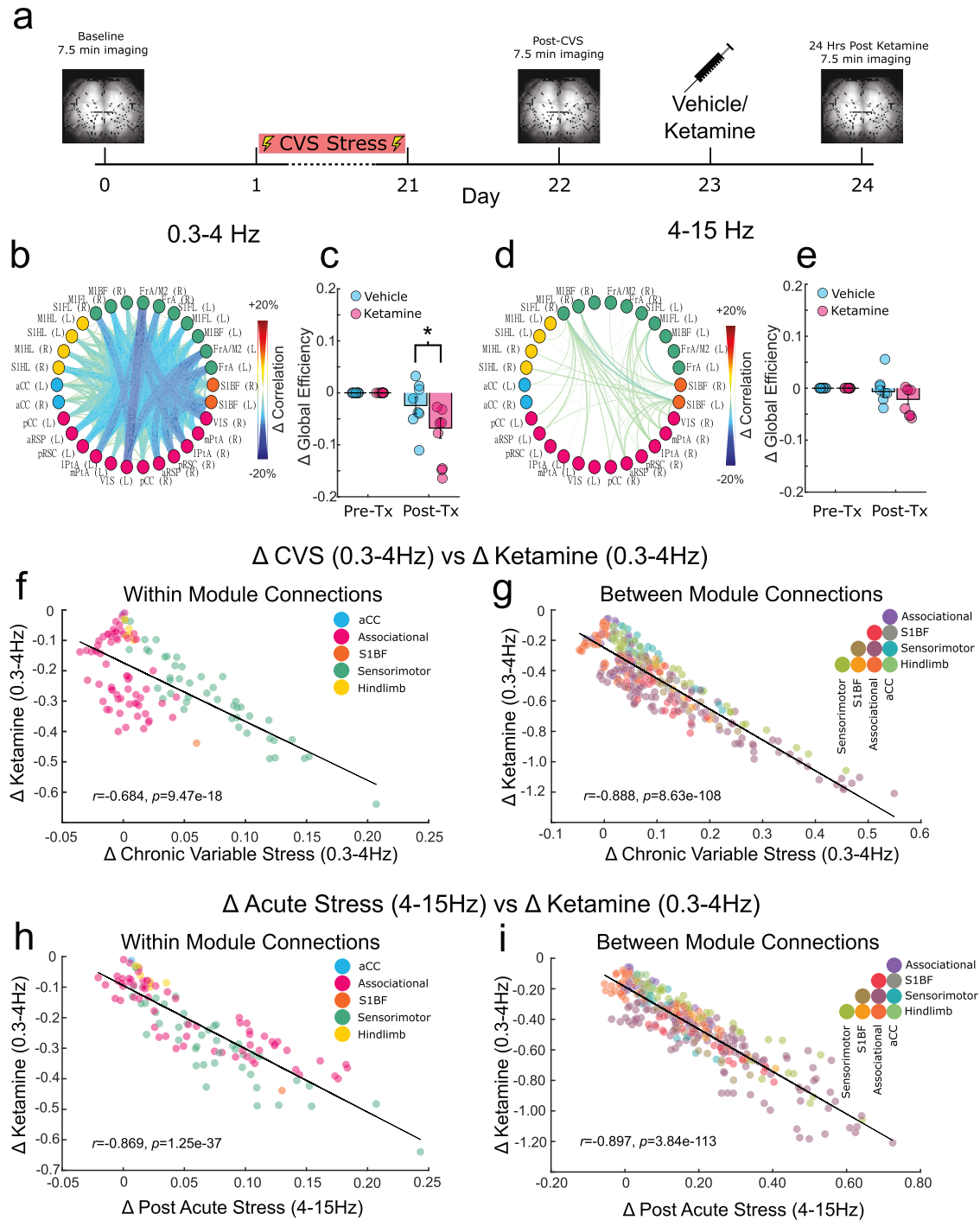


Fig. 5 Ketamine reverses functional connectivity changes after chronic stress in the 0.3–4 Hz band. **a** Experiment diagram. After 21 day CVS and a post-stress imaging session, mice were administered ketamine, and 24 h later imaged in a post-Ketamine session. **b** Biograph displaying the change in strength of connections in the 0.3–4 Hz band 24 h after ketamine treatment ($n = 8$) relative to connection strength after CVS. Between-module connections were significantly reduced 24 h after ketamine treatment relative to a vehicle injection ($n = 8$). **c** Global efficiency of the network in the 0.3–4 Hz band was significantly reduced 24 h after ketamine treatment relative to a vehicle injection. **d** Biograph displaying the change in strength of connections in the 4–15 Hz band 24 h after ketamine treatment relative to connection strength after CVS. Between-module connections and within-module connections were unchanged. **e** Global efficiency was not significantly reduced in the 4–15 Hz band 24 h after ketamine treatment relative to a vehicle injection. Connection-specific correlation changes after ketamine treatment were negatively correlated to the changes observed due to chronic stress. **f** Within modules, a strong negative correlation was observed between connection strength changes after ketamine in the 0.3–4 Hz band and connection strength changes after chronic stress. **g** Between modules, a strong negative correlation was observed between connection strength changes after ketamine treatment and connection strength changes after chronic stress. Acute stress connection strength changes in the 4–15 Hz band were highly negatively correlated both within modules (**h**) and between modules (**i**) with changes due to ketamine treatment. (* $p < 0.05$, ** $p < 0.01$, *** $p < 0.001$ follow-up pairwise comparison or Pearson correlation).

Functional connectivity represents the sum of coordinated activity that occurs as a result of direct and indirect anatomical connectivity [39], and the physiological response to a single stressor is an ordered neurochemical cascade that has synaptic, cellular, and behavioral effects [40]. Notably, early phases of the response involving monoamines and prolonged responses involving glucocorticoids in response to psychogenic or physical stress collectively mediate neuronal activity and synaptic plasticity changes in the cortex [7]. It is possible that the rapid evolution of the acute functional connectivity changes, and their long-term repercussions, are related to this ordered cascade. Acute stress elevates extracellular glutamate [41–43], glutamate receptors [44] and corticosterone treatment elevates mEPSC frequency and PPF in slice [45]. Our data here suggest that stress mediated changes in cortical neuronal function extend well beyond the prefrontal cortex and produce widespread alterations in cortical communication. Future work will elucidate the mechanisms that contribute to the acute changes in functional connectivity.

Subanesthetic ketamine provides a unique window for capturing large scale functional network changes resulting from rapid synaptogenesis. It results in rapid changes in key emotional and cognitive circuits [25, 46, 47], in addition to global increases in trophic factors [46]. These changes may be contingent on glutamate bursting that we have previously described [14], and increasing data suggests that synaptogenesis after subanesthetic ketamine is not stochastic [26].

Our results here are limited to male mice. Sexual dimorphism in the response to stress and models of depression are well-documented [48], consistent with sex-mediated differences in clinical populations. Moreover, functional connectivity differences between males and females with major depressive disorder are increasingly recognized [49]. Accordingly, sex-specific relationships between acute and chronic stress reorganization will require dedicated study.

CONCLUSION

Our data indicates that stress induces functional connectivity changes with spatiotemporal features that link acute stress, persistent network reorganization after chronic stress, and treatment effects. Parallels between these canonically dichotomized states may inform the investigation of allostatic load in health and disease. Additional study is required to understand how allostasis is associated with the instantiation of acute stress phenotypes across different temporal bands, and how structural plastic changes recruited by repeated stress events specifically remodel large scale networks to potentially anticipate and prepare for stress.

DATA AVAILABILITY

The datasets generated and analysed for the current study are available from the corresponding author on reasonable request.

REFERENCES

1. WHO. (ed Department of Health Statistics and Informatics) (WHO Press, Geneva, 2008).
2. McEwen BS. Mood disorders and allostatic load. *Biol Psychiatry*. 2003;54:200–7.
3. Kaiser RH, Andrews-Hanna JR, Wager TD, Pizzagalli DA. {Large-Scale} Network dysfunction in major depressive disorder: a meta-analysis of {Resting-State} functional connectivity. *JAMA Psychiatry*. 2015;72:603–11.
4. Gong Q, He Y. Depression, neuroimaging and connectomics: a selective overview. *Biol Psychiatry*. 2015;77:223–35.
5. Menon V. Large-scale brain networks and psychopathology: a unifying triple network model. *Trends Cogn Sci*. 2011;15:483–506.
6. Willner P. Validity, reliability and utility of the chronic mild stress model of depression: a 10-year review and evaluation. *Psychopharmacology*. 1997;134:319–29.

7. Popoli M, Yan Z, McEwen BS, Sanacora G. The stressed synapse: the impact of stress and glucocorticoids on glutamate transmission. *Nat Rev Neurosci*. 2012;13:22–37.
8. Cook SC, Wellman CL. Chronic stress alters dendritic morphology in rat medial prefrontal cortex. *J Neurobiol*. 2004;60:236–48.
9. Liston C, Gan WB. Glucocorticoids are critical regulators of dendritic spine development and plasticity in vivo. *Proc Natl Acad Sci USA*. 2011;108:16074–9.
10. Henckens MJ, van der Marel K, van der Toorn A, Pillai AG, Fernández G, Dijkhuizen RM, et al. Stress-induced alterations in large-scale functional networks of the rodent brain. *Neuroimage*. 2015;105:312–22.
11. Nephew BC, Huang W, Poirier GL, Payne L, King JA. Altered neural connectivity in adult female rats exposed to early life social stress. *Behavioural Brain Res*. 2017;316:225–33.
12. Gass N, Becker R, Schwarz AJ, Weber-Fahr W, Clemm von Hohenberg C, Vollmayr B, et al. Brain network reorganization differs in response to stress in rats genetically predisposed to depression and stress-resilient rats. *Transl Psychiatry*. 2016;6:e970.
13. Nakayama R, Ikegaya Y, Sasaki T. Cortical-wide functional correlations are associated with stress-induced cardiac dysfunctions in individual rats. *Sci Rep*. 2019;9:1–10.
14. McGirr A, LeDue J, Chan AW, Xie Y, Murphy TH. Cortical functional hyperconnectivity in a mouse model of depression and selective network effects of ketamine. *Brain*. 2017;140:2210–25.
15. Ferris CF, Stolberg T. Imaging the immediate non-genomic effects of stress hormone on brain activity. *Psychoneuroendocrinology*. 2010;35:5–14.
16. Berretz G, Packheiser J, Kumsta R, Wolf OT, Ockenburg S. The brain under stress—A systematic review and activation likelihood estimation meta-analysis of changes in BOLD signal associated with acute stress exposure. *Neurosci Biobehav Rev*. 2021;124:89–99.
17. Maron-Katz A, Vaisvaser S, Lin T, Hendler T, Shamir R. A large-scale perspective on stress-induced alterations in resting-state networks. *Sci Rep*. 2016;6:21503.
18. Zhang W, Hashemi MM, Kaldewaij R, Koch S, Beckmann C, Klumpers F, et al. Acute stress alters the 'default' brain processing. *Neuroimage*. 2019;189:870–7.
19. Lu H, Zou Q, Gu H, Raichle ME, Stein EA, Yang Y. Rat brains also have a default mode network. *Proc Natl Acad Sci*. 2012;109:3979–84.
20. Silasi G, Xiao D, Vanni MP, Chen ACN, Murphy TH. Intact skull chronic windows for mesoscopic wide-field imaging in awake mice. *J Neurosci Methods*. 2016;267:141–9.
21. Chen T-W, Wardill TJ, Sun Y, Pulver SR, Renninger SL, Baohan A, et al. Ultra-sensitive fluorescent proteins for imaging neuronal activity. *Nature*. 2013;499:295–300.
22. Lim DH, LeDue JM, Murphy TH. Network analysis of mesoscale optical recordings to assess regional, functional connectivity. *Neurophotonics*. 2015;2:041405.
23. Ma Y, Shaik MA, Kim SH, Kozberg MG, Thibodeaux DN, Zhao HT, et al. Wide-field optical mapping of neural activity and brain haemodynamics: considerations and novel approaches. *Philos Trans R Soc Lond B Biol Sci*. 2016;371:20150360.
24. Dana H, Novak O, Guardado-Montesino M, Franssen JW, Hu A, Borghuis BG, et al. Thy1 transgenic mice expressing the red fluorescent calcium indicator {jRGECO1a} for neuronal population imaging in vivo. *PLoS One*. 2018;13:e0205444.
25. Li N, Lee B, Liu RJ, Banasr M, Dwyer JM, Iwata M, et al. mTOR-dependent synapse formation underlies the rapid antidepressant effects of NMDA antagonists. *Science*. 2010;329:959–64.
26. Moda-Sava RN, Murdock MH, Parekh PK, Fetcho RN, Huang BS, Huynh TN, et al. Sustained rescue of prefrontal circuit dysfunction by antidepressant-induced spine formation. *Science*. 2019;364:eaat8078.
27. Thériault RK, Manduca JD, Perreault ML. Sex differences in innate and adaptive neural oscillatory patterns link resilience and susceptibility to chronic stress in rats. *J Psychiatry Neurosci*. 2021;46:E258–70.
28. Labonté B, Engmann O, Purushothaman I, Menard C, Wang J, Tan C, et al. Sex-specific transcriptional signatures in human depression. *Nat Med*. 2017;23:1102–11.
29. LaPlant Q, Chakravarty S, Vialou V, Mukherjee S, Koo JW, Kalahasti G, et al. Role of nuclear factor κ B in ovarian hormone-mediated stress hypersensitivity in female mice. *Biol Psychiatry*. 2009;65:874–80.
30. Gould TD, Dao DT & Kovacs CE. The open field test. Mood and anxiety related phenotypes in mice, 2009; 1–20.
31. Dulawa SC. Novelty-induced hypophagia. Mood and anxiety related phenotypes in mice, 2009;247–59.
32. Rubinov M, Sporns O. Complex network measures of brain connectivity: uses and interpretations. *Neuroimage*. 2010;52:1059–69.
33. Wang Q, Ding SL, Li Y, Royall J, Feng D, Lesnar P, et al. The Allen mouse brain common coordinate framework: a 3D reference atlas. *Cell*. 2020;181:936–953. e920.
34. Mohajerani MH, Chan AW, Mohsenvand M, LeDue J, Liu R, McVea DA, et al. Spontaneous cortical activity alternates between motifs defined by regional axonal projections. *Nat Neurosci*. 2013;16:1426–35.

35. Hodes GE, Pfau ML, Leboeuf M, Golden SA, Christoffel DJ, Bregman D, et al. Individual differences in the peripheral immune system promote resilience versus susceptibility to social stress. *Proc Natl Acad Sci*. 2014;111:16136–41.
36. Singh JB, Fedgchin M, Daly EJ, De Boer P, Cooper K, Lim P, et al. A double-blind, randomized, placebo-controlled, dose-frequency study of intravenous ketamine in patients with treatment-resistant depression. *Am J Psychiatry*. 2016;173:816–26.
37. Maeng S, Zarate CA Jr, Du J, Schloesser RJ, McCammon J, Chen G, et al. Cellular mechanisms underlying the antidepressant effects of ketamine: role of α -amino-3-hydroxy-5-methylisoxazole-4-propionic acid receptors. *Biol Psychiatry*. 2008;63:349–52.
38. McEwen BS. Physiology and neurobiology of stress and adaptation: central role of the brain. *Physiol Rev*. 2007;87:873–904.
39. Wang Z, Chen LM, Négyessy L, Friedman RM, Mishra A, Gore JC, et al. The relationship of anatomical and functional connectivity to resting-state connectivity in primate somatosensory cortex. *Neuron*. 2013;78:1116–26.
40. Joëls M, Baram TZ. The neuro-symphony of stress. *Nat Rev Neurosci*. 2009;10:459–66.
41. Moghaddam B. Stress preferentially increases extraneuronal levels of excitatory amino acids in the prefrontal cortex: comparison to hippocampus and basal ganglia. *J Neurochem*. 1993;60:1650–7.
42. Hascup ER, Hascup KN, Stephens M, Pomerleau F, Huettl P, Gratton A, et al. Rapid microelectrode measurements and the origin and regulation of extracellular glutamate in rat prefrontal cortex. *J Neurochem*. 2010;115:1608–20.
43. Musazzi L, Milanese M, Farisello P, Zappettini S, Tardito D, Barbiero VS, et al. Acute stress increases depolarization-evoked glutamate release in the rat prefrontal/ frontal cortex: the dampening action of antidepressants. *PLoS One*. 2010;5:e8566.
44. Yuen EY, Liu W, Karatsoreos IN, Feng J, McEwen BS, Yan Z. Acute stress enhances glutamatergic transmission in prefrontal cortex and facilitates working memory. *Proc Natl Acad Sci*. 2009;106:14075–9.
45. Karst H, Berger S, Turiault M, Tronche F, Schütz G, Joëls M. Mineralocorticoid receptors are indispensable for nongenomic modulation of hippocampal glutamate transmission by corticosterone. *Proc Natl Acad Sci*. 2005;102:19204–7.
46. Autry AE, Adachi M, Nosyreva E, Na ES, Los MF, Cheng PF, et al. NMDA receptor blockade at rest triggers rapid behavioural antidepressant responses. *Nature*. 2011;475:91–5.
47. Carreno FR, Donegan JJ, Boley AM, Shah A, DeGuzman M, Frazer A, et al. Activation of a ventral hippocampus-medial prefrontal cortex pathway is both necessary and sufficient for an antidepressant response to ketamine. *Mol Psychiatry*. 2016;21:1298–308.
48. Pfau ML, Russo SJ. Peripheral and central mechanisms of stress resilience. *Neurobiol Stress*. 2015;1:66–79.
49. Talishinsky A, Downar J, Vértes PE, Seidlitz J, Dunlop K, Lynch CJ, et al. Regional gene expression signatures are associated with sex-specific functional connectivity changes in depression. *Nat Commun*. 2022;13:1–20.

ACKNOWLEDGEMENTS

We thank Kylie Meir for technical assistance.

AUTHOR CONTRIBUTIONS

DMA & AM conceived of the study, conducted experiments, analyzed data, and wrote the manuscript.

FUNDING

This study was funded through the Campus Alberta Innovates Program Chair in Neurostimulation to AM. DMA is supported by a Canadian Open Neuroscience Platform (CONP) Scholar Award.

COMPETING INTERESTS

The authors declare no competing interests.

ADDITIONAL INFORMATION

Supplementary information The online version contains supplementary material available at <https://doi.org/10.1038/s41386-022-01506-y>.

Correspondence and requests for materials should be addressed to Alexander McGirr.

Reprints and permission information is available at <http://www.nature.com/reprints>

Publisher's note Springer Nature remains neutral with regard to jurisdictional claims in published maps and institutional affiliations.

Springer Nature or its licensor (e.g. a society or other partner) holds exclusive rights to this article under a publishing agreement with the author(s) or other rightsholder(s); author self-archiving of the accepted manuscript version of this article is solely governed by the terms of such publishing agreement and applicable law.